

Weakly Supervised Visual Semantic Parsing

Alireza Zareian, Svebor Karaman, and Shih-Fu Chang
Columbia University, New York, NY, USA

{az2407, sk4089, sc250}@columbia.edu

Abstract

Scene Graph Generation (SGG) aims to extract entities, predicates and their intrinsic structure from images, leading to a deep understanding of visual content, with many potential applications such as visual reasoning and image retrieval. Nevertheless, computer vision is still far from a practical solution for this task. Existing SGG methods require millions of manually annotated bounding boxes for scene graph entities in a large set of images. Moreover, they are computationally inefficient, as they exhaustively process all pairs of object proposals to predict their relationships. In this paper, we address those two limitations by first proposing a generalized formulation of SGG, namely Visual Semantic Parsing, which disentangles entity and predicate prediction, and enables sub-quadratic performance. Then we propose the Visual Semantic Parsing Network, VSPNET, based on a novel three-stage message propagation network, as well as a role-driven attention mechanism to route messages efficiently without a quadratic cost. Finally, we propose the first graph-based weakly supervised learning framework based on a novel graph alignment algorithm, which enables training without bounding box annotations. Through extensive experiments on the Visual Genome dataset, we show VSPNET outperforms weakly supervised baselines significantly and approaches fully supervised performance, while being five times faster.

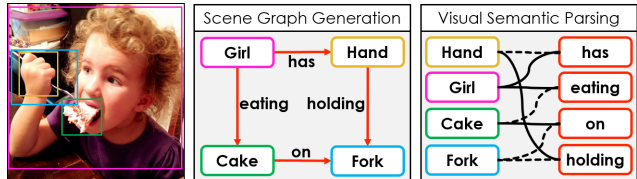


Figure 1. An illustration of a structured visual knowledge extraction formulated as a Scene Graph Generation with predicates as edges or as a Visual Semantic Parsing with predicates as nodes and roles as edges.

of Scene Graph Generation (SGG) aims to represent an image with a set of entities (nodes) and relations (directed edges). Figure 1 (center) illustrates an example from the Visual Genome [11] dataset. Several methods have been proposed to address this problem which have achieved great performance on challenging benchmarks. Nevertheless, important challenges remain unaddressed. Most existing methods operate on a fully connected graph that quadratically grows with the number of region proposals. Extending to higher-order relationships (e.g. *girl eating cake with fork*) would make this problem even more expensive. Furthermore, most existing methods require bounding box annotation for each object that embodies a node in the ground truth graph, which is an expensive constraint.

Considering the importance of structured parsing for computer vision, we propose a Visual Semantic Parsing Network (VSPNET), which aim to address the two mentioned limitations, *i.e.*, computation and supervision costs. To this end, we generalize the formulation of SGG to represent predicates (relations) as nodes in the same semantic space as entity nodes, and instead, represent semantic *roles* (e.g. subject and object) as edges. Figure 1 (right) illustrates the structured extraction following this *Visual Semantic Parsing* (VSP) formalism with subject edges depicted with solid lines and object edges with dashed lines. This not only allows us to break the quadratic complexity, but also can support higher-order relationships that cannot be expressed using the existing SGG formulation. Based on the VSP formulation, we propose a dynamic attentional message passing network that iteratively infers node representations and role connections, resulting in a scene graph.

1. Introduction

Contemporary neural networks have excelled in various tasks once exclusive to humans, such as visual object detection [23], and text translation [1]. However, they still fall short of tasks which require deeper data understanding and cognitive abilities, such as visual question answering (VQA) [35]. Motivated by the success of structured information extraction in natural language processing ([2], [24]), computer vision has started to adopt structured representations to improve performance and explainability in various tasks such as VQA [27, 25] as well as image retrieval [8]. Towards structured visual information extraction, the task

Our proposed method consists of a novel three-stage message aggregation network, along with a *role-driven* attention mechanism to route messages efficiently throughout the graph. The proposed architecture does not need to process all pairs of region proposals and hence is computationally efficient. In order to define a differentiable objective function to train our VSPNET in the weakly supervised setting, we also propose a novel graph alignment technique. Through extensive experiments on the Visual Genome dataset, we show that VSPNET achieves significantly higher accuracy compared to weakly supervised counterparts, approaching fully supervised baselines. We also show the proposed method is easily adaptable to the supervised setting, while maintaining the computational efficiency. Finally, we experimentally show that our method is 5 times faster than the most efficient baseline. We publicly release the source code of our method¹.

2. Related work

In this section we give an overview of structured visual representation in the computer vision literature, covering scene graph generation and other relevant tasks. Then we provide a detailed summary of the SGG methods, followed by a review of other computer vision methods that use graphical message passing models like ours.

2.1. Structured visual representation

Computer vision has made impressive progress on unstructured prediction tasks such as image classification and object detection. However, extracting a set of entities or predicates from an image does not result in a full understanding, unless we also extract the relationships between entities and the roles they play for each predicate. Visual Relation Detection (VRD) [17, 37, 38, 15, 5, 21, 33, 39, 32, 7, 20] aims to classify relationships between each pair of detected objects in a scene. These relations include verbs as well as other types of relationship such as comparative and spatial. More recently, Scene Graph Generation (SGG) [29] redefines VRD as a problem of jointly detecting objects and their relationships.

Nevertheless, critical challenges remain in this field. The task of SGG requires drawing an exact bounding box around each object, which is why existing methods require a training dataset where every node of the ground truth graphs comes with a manually annotated bounding box. Although such a dataset is available (Visual Genome), it is limited to 150 object classes and 50 relation classes. Applications that involve other classes would require expensive manual labor. Bounding box localization is an independent task involving low-level boundary analysis rather than high-level semantic reasoning. We should thus ideally disentangle it from SGG,

¹The code will be released upon acceptance.

such that localization is learned separately, and SGG does not need localized ground truth graphs for training. Zhang *et al.* [38] recently proposed the only Weakly Supervised VRD method successfully applied on the Visual Genome SGG task. However, the performance is far from fully supervised counterparts. In this paper we try to close this gap, reporting a significant advancement in Section 4.

2.2. Scene graph generation

The majority of SGG methods start by extracting region proposals from the input image, perform some kind of information propagation to incorporate context, and then classify each region to an object class, as well as each pair of regions to a relation class [29, 14, 36, 13, 28]. They start with a fully connected graph formed by hundreds of regions, and prune it by classifying each non-existent node or edge to a background class. This process has a quadratic order and is thus inefficient. Recently, [30] tried to reduce the computational complexity by first pruning the graph using a light-computation model and then processing the remaining graph by a heavy-computation model. However, this does not eliminate the quadratic order of computations. In contrast, we do not start from a fully connected graph but instead, select a limited number of edges using a (sub-quadratic) attention module and only process those.

Newell and Deng [19] proposed to not rely on region proposals at all, but operating on two grids of feature maps, representing entities and predicates. Our method is similar to theirs in that we consider a constant number of predicates and infer their connection to entities, rather than processing all pairs of entities. In contrast with [19] though, we still utilize region proposals as our entity nodes and employ message passing to incorporate context.

2.3. Message passing in computer vision

Recent deep learning models have increasingly utilized message passing in various computer vision tasks. [16, 3, 9]. Given a graph where nodes are represented by feature vectors, message passing networks iteratively update the features of each node by applying a neural function on the node’s current features as well as its neighbors’. Most SGG methods use message passing to propagate information between region proposals [29, 14, 13, 30]. Instead of propagating messages through a static, often fully-connected graph, we use a differentiable, weighted graph that is directly supervised to emphasize the messages passed between relevant entity-predicate pairs.

The most similar to our framework is that of [34] and [22], as they do not rely on a static graph with fixed edges but iteratively update the edges between message passing steps. Qi *et al.* [22] define a fully connected weighted graph connecting all pairs of region proposals in an image, upon which they perform message passing. The edge

weights are updated iteratively between message passing steps. They use the final graph to classify humans, objects and their interactions. While they demonstrate promising results, their method still suffers from the quadratic order. Yuan *et al.* [34] employ a similar approach for object classification in videos. We use a similar interleaved node and edge inference framework, but edges are between entities and predicates rather than pairs of entities, which results in computational efficiency. Furthermore, we define multiple types of edges, corresponding to different semantic roles, and use dedicated parameters for each edge type to propagate role-driven messages. To handle potentially large graphs, we propose a three-stage message aggregation network that carefully inserts incoming messages to each node.

3. Method

In this section, we first formalize our problem in Section 3.1, then detail our method and its two-fold contributions: the VSPNET architecture for constructing a semantic graph from an image (Section 3.2), and a graph alignment algorithm for weakly supervised training of the proposed network (Section 3.3). Figure 2 illustrates the general pipeline of our method.

3.1. Problem formulation

Given an image I , the goal of SGG is to produce a graph $G_{\text{SGG}} = (\mathcal{N}, \mathcal{E})$ where each node in \mathcal{N} is represented by an entity class $c_i \in \mathcal{C}_e$ and a bounding box b_i , and the set of edges assign a predicate class (including background) to each directed pair of nodes, *i.e.*, $\mathcal{E} : \mathcal{N} \times \mathcal{N} \mapsto \mathcal{C}_p \cup \{\emptyset\}$. Conceptually, an edge associates each predicate to a pair of entities, in the order they would appear in an English caption (*e.g.* *person sitting on chair* would be represented as an edge labeled *sitting on*, going from the node *person* to the node *chair*, and not the other way).

Nevertheless, this notation is inherently limiting, as it restricts predicates to have exactly two arguments present in the scene. This constraint may be acceptable for relational predicates such as prepositions, but certainly not for verbs, which constitute an important group of predicates. To relax this constraint, we follow [31] to adopt the formulation of Semantic Role Labeling (SRL) from NLP. In SRL, predicates are represented as nodes, and edges represent semantic roles that entities play in each predicate. Applying the SRL formalism to the scene graph generation task we can define Visual Semantic Parsing (VSP) as having the goal of predicting a graph $G_{\text{VSP}} = (\mathcal{N}_e, \mathcal{N}_p, \mathcal{E})$, where

$$\begin{aligned} \mathcal{N}_e &= \left\{ (c_i \in \mathcal{C}_e, b_i \in \mathbb{R}^4) \right\}_{i=1}^{n_e}, \\ \mathcal{N}_p &= \{c_k \in \mathcal{C}_p\}_{k=1}^{n_p}, \text{ and} \\ \mathcal{E} &: \mathcal{N}_p \times \mathcal{N}_e \mapsto \mathcal{C}_r \cup \{\emptyset\}. \end{aligned} \quad (1)$$

Every scene graph G_{SGG} has an equivalent VSP graph G_{VSP} where the set of role classes \mathcal{C}_r has two members: head and tail of the relation edge, *i.e.*, subject and object. However, an arbitrary VSP graph does not necessarily map to a scene graph, as a predicate may connect to less or more than two entities, potentially involving more than two semantic role types. Hence, VSP is a generalization of SGG.

In this paper we employ the VSP formalism, not only because it covers a wider range of semantics, but also because it naturally leads to a more efficient model architecture. Indeed, in order to consider all possible relationships, most existing methods process a fully connected graph with n_e^2 edges, where n_e is usually the number of proposals which is typically 300. This is while more than 99% of graphs in Visual Genome have less than 20 predicates (edges), and the largest one has 53. It is not possible to prune the n_e^2 edges without processing them all, but the VSP formalism circumvents this burden. We consider predicates to be nodes rather than edges, and instead of n_e^2 predicate nodes, we allocate a constant number of them n_p , far less than n_e^2 .

3.2. Visual semantic parsing network

Given an image and n_e region proposals, we initialize a VSP graph with n_e entity nodes, initially represented by proposal features, and n_p predicate nodes, with random initial states. First, a novel role-driven attention module is devised to compute n_r association scores between entity-predicate pairs, each estimating the likelihood of a certain semantic role. Then, our three-stage message aggregation network is employed to propagate messages through weighted edges (n_r) predicted in the previous step, updating node states, resulting in a contextualized representation. This process is repeated for a fixed number of iterations, successively updating nodes and edges. We use the final states of entity and predicate nodes to classify their semantic categories, and use the final attention scores to determine the semantic roles.

Formally, we define $H_e^{(0)} \in \mathbb{R}^{n_e \times d_e}$ to be the initial hidden state of n_e entity nodes, and initialize each row with the appearance (RoI [23]) feature of the corresponding region proposal, concatenated with its bounding box coordinates. We also define $H_p^{(0)} \in \mathbb{R}^{n_p \times d_p}$ to be the initial hidden state of n_p predicate nodes. $H_p^{(0)}$ is a trainable matrix, randomly initialized before training but fixed during test. Given $H_e^{(t)}$ and $H_p^{(t)}$, we compute a set of role-driven attention matrices $A_r^{(t)} \in \mathbb{R}^{n_p \times n_e}$, each representing a semantic role class r in \mathcal{C}_r .

$$A_r^{(t)}[k, i] = \frac{\hat{A}_r^{(t)}[k, i]}{p_\emptyset + \sum_{i'=1}^{n_e} \hat{A}_r^{(t)}[k, i']} \quad (2)$$

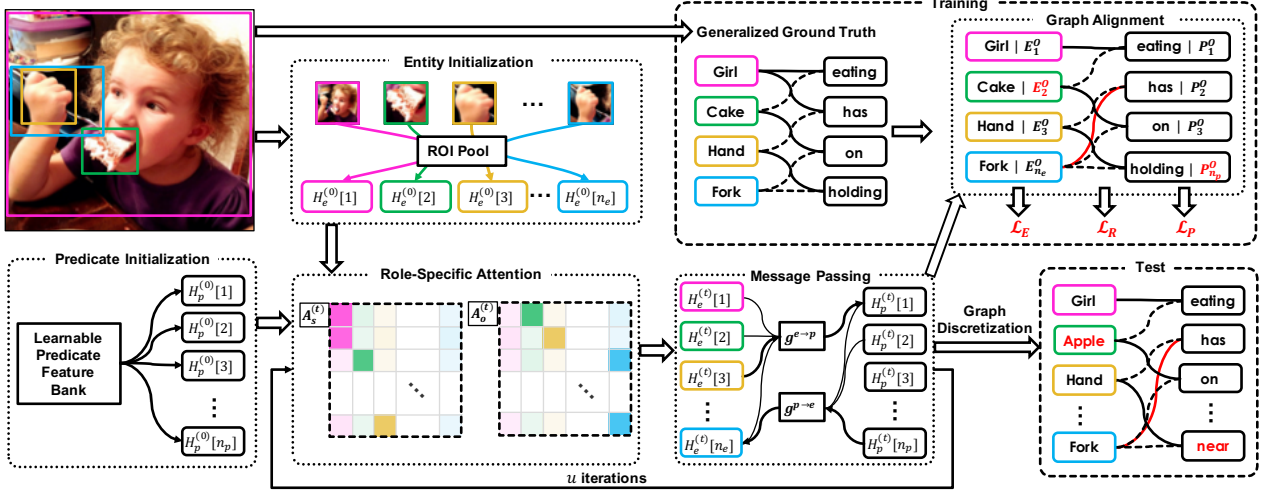


Figure 2. Overview of our proposed framework: given an input image and region proposals, a scene graph is produced by an iterative process involving a multi-headed attention module that infers connections between entities and predicates nodes, and a message passing module to propagate information between nodes and update their states. To compute our losses on nodes and edges during training, the unlocalized ground truth is aligned to our output graph. Best viewed in color.

where

$$\hat{A}_r^{(t)}[k, i] = \exp\left(f_r\left([H_p^{(t)}[k] \parallel H_e^{(t)}[i]\right]\right), \quad (3)$$

$[\cdot]$ represents concatenation, $H[k]$ represents the k th row of H , and f_r is a trainable fully connected network. Moreover, p_\emptyset is a constant that makes it possible for a predicate to take neither of the entities for a certain role.

After computing attention matrices, we use them to propagate contextual information from a predicate to its relevant entities and vice versa. We update the node states by message passing across the edges. To this end, we compute the incoming message to each entity, using a three-stage aggregation mechanism:

$$\begin{aligned} M_e^{(t)}[i] &= g^{p \rightarrow e}(A^{(t)}, H_p^{(t)}) \\ &= g^e\left(\sum_{r=1}^{n_r} g_r^{e \leftarrow} \left(\sum_{k=1}^{n_p} A_r^{(t)}[k, i] g_r^{p \rightarrow}(H_p^{(t)}[k])\right)\right), \end{aligned} \quad (4)$$

where $g_r^{p \rightarrow}$ computes the outgoing message from each predicates for the r th edge type, $g_r^{e \leftarrow}$ computes the incoming message from all predicates to each entity for the r th role, and finally g^e aggregates messages across role types. All three functions are trainable fully connected networks. Similarly, the incoming message for a predicate is

$$\begin{aligned} M_p^{(t)}[k] &= g^{e \rightarrow p}(A^{(t)}, H_e^{(t)}) \\ &= g^p\left(\sum_{r=1}^{n_r} g_r^{p \leftarrow} \left(\sum_{i=1}^{n_e} A_r^{(t)}[k, i] g_r^{e \rightarrow}(H_e^{(t)}[i])\right)\right). \end{aligned} \quad (5)$$

After collecting messages for each node, we update their

state using two Gated Recurrent Units (GRU) [4].

$$\begin{aligned} H_e^{(t+1)}[i] &= \text{GRU}_e\left(H_e^{(t)}[i], M_e^{(t)}[i]\right), \text{ and} \\ H_p^{(t+1)}[k] &= \text{GRU}_p\left(H_p^{(t)}[k], M_p^{(t)}[k]\right). \end{aligned} \quad (6)$$

This process is repeated for a constant number of times u , and the final states $H_e^{(u)}$ and $H_p^{(u)}$ are passed through another pair of fully connected networks (h_e, h_p) to produce semantic embeddings E^O and P^O for entity and predicate nodes. The final state of the adjacency matrices $A_r^{(u)}$ are stacked together and named A^O .

After the message passing process, we have a continuous and fully differentiable output graph $G_{\text{soft}}^O = (E^O, P^O, A^O)$. In order to produce a valid, discrete graph as defined in (1), we apply the following two post-processing steps, also referred to as the discretization process. First, we convert E^O and P^O to discrete labels by picking the nearest neighbor of each of their rows among a dictionary of entity and predicate class embeddings. Next, we binarize the fully connected attention matrices A_r^O by setting the max value in each row to 1 and the rest to 0. This is to ensure each predicate has only one entity for each semantic role c_r . This leads to a discrete graph $G^O = (\mathcal{N}_e^O, \mathcal{N}_p^O, \mathcal{E}^O)$.

In the next subsection, we define our cost function, where we also need the opposite process: converting a ground truth graph $G^T = (\mathcal{N}_e^T, \mathcal{N}_p^T, \mathcal{E}^T)$ to a soft representation $G_{\text{soft}}^T = (E^T, P^T, A^T)$. To this end, we stack the class embedding of entity and predicate nodes to get matrices E^T and P^T , and encode the edges into a binary adjacency matrix A^T .

3.3. Training

We train our model using pairs of image and unlocalized ground truth graph. Specifically, we need to compare the soft output graph G_{soft}^O (*i.e.* before discretization) to the target G_{soft}^T to calculate a differentiable cost to be minimized. To define a differentiable graph matching cost, we first find an alignment (*i.e.*, nodes correspondence) between the two graphs, and then define the overall cost as a summation of nodes and edges costs.

3.3.1 Learning objective

Formally, we define an alignment \mathcal{I} between the output and target graphs as:

$$\begin{aligned} \mathcal{I} &= (\mathcal{I}_e, \mathcal{I}_p), \text{ where} \\ \mathcal{I}_e &= \{(i, j) | i \in \{1 \dots n_e^O\}, j \in \{1 \dots n_e^T\}\}, \text{ and} \\ \mathcal{I}_p &= \{(k, l) | k \in \{1 \dots n_p^O\}, l \in \{1 \dots n_p^T\}\}, \end{aligned} \quad (7)$$

such that for any i there is at most one j , and for each j , there is at most one i , such that $(i, j) \in \mathcal{I}_e$, and similarly for the predicates alignment \mathcal{I}_p . In practice, the number of entities n_e^O and n_p^O are the same as the numbers n_e and n_p in the previous section, but could be lower in theory if any filtering is applied to the output graph. In order to maximize supervision, we want to align as many nodes as possible from the output graph to the target graph. Therefore, we constrain \mathcal{I} such that

$$\begin{aligned} |\mathcal{I}_e| &= \min(n_e^O, n_e^T), \text{ and} \\ |\mathcal{I}_p| &= \min(n_p^O, n_p^T), \end{aligned} \quad (8)$$

where $|\cdot|$ denotes set cardinality. Given an alignment \mathcal{I} between output and target graphs, we define our overall cost function \mathcal{L} as

$$\mathcal{L}(G^O, G^T, \mathcal{I}) = \mathcal{L}_E + \mathcal{L}_P + \lambda \mathcal{L}_R, \quad (9)$$

which is a combination of costs for entity recognition, predicate recognition, and semantic role inference. We define the entity loss \mathcal{L}_E and predicate loss \mathcal{L}_P to be the mean square errors on entity and predicate embeddings, and the role connections loss \mathcal{L}_R to be a binary cross entropy loss on all attention scores. More specifically, the entity loss is

$$\mathcal{L}_E(G^O, G^T, \mathcal{I}) = \frac{1}{|\mathcal{I}_e|} \sum_{(i,j) \in \mathcal{I}_e} \|E_i^O - E_j^T\|_2^2, \quad (10)$$

and similarly the predicate loss is

$$\mathcal{L}_P(G^O, G^T, \mathcal{I}) = \frac{1}{|\mathcal{I}_p|} \sum_{(k,l) \in \mathcal{I}_p} \|P_k^O - P_l^T\|_2^2. \quad (11)$$

We define the single role matching cost for role r as

$$\mathcal{L}_r = \frac{1}{|\mathcal{I}|} \sum_{(i,j) \in \mathcal{I}_e} \sum_{(k,l) \in \mathcal{I}_p} \mathcal{X}(A_r^O[k, i], A_r^T[l, j]), \quad (12)$$

where $|\mathcal{I}| = |\mathcal{I}_e| |\mathcal{I}_p|$, and $\mathcal{X}(p, q)$ is the binary cross entropy function, *i.e.*,

$$\mathcal{X}(p, q) = -q \log p - (1 - q) \log(1 - p). \quad (13)$$

We then define the overall role connections loss as

$$\mathcal{L}_R(G^O, G^T, \mathcal{I}) = \frac{1}{n_r} \sum_{r=1}^{n_r} \mathcal{L}_r \quad (14)$$

Since \mathcal{L}_R is in a different scale than \mathcal{L}_E and \mathcal{L}_P , we use a hyperparameter λ to balance its significance in the overall loss defined in (9).

Since the alignment is not known in the weakly supervised setting, our training involves the following nested optimization

$$\phi^* = \underset{\phi}{\operatorname{argmin}} \mathbb{E} \left[\min_{\mathcal{I}} \mathcal{L}(G^O, G^T, \mathcal{I}) \right], \quad (15)$$

where ϕ is the collection of model parameters that lead to G^O , and the expectation is estimated by averaging over training data. Note that the inner optimization is subject to the constraints in (8). Section 3.3.2 describes how the inner optimization is solved. We use the Adam Optimizer [10] for the outer optimization. Note that existing SGG methods do not entail the inner optimization since they align² the entity nodes based on their bounding box overlap with the ground truth. This is not possible in our weakly supervised settings, as we do not have access to ground truth bounding boxes.

3.3.2 Graph alignment

There are no efficient exact algorithms for solving the inner optimization in (15). Hence, we propose an iterative algorithm to approximate the optimal alignment. We show that given an entity alignment \mathcal{I}_e , it is possible to find the optimal predicate alignment \mathcal{I}_p in polynomial time, and similarly from \mathcal{I}_p to \mathcal{I}_e . Accordingly, we propose an alternating optimization algorithm with guaranteed convergence to a local optima. Supposing \mathcal{I}_e is given, we intend to find \mathcal{I}_p that minimizes \mathcal{L} . Since \mathcal{L}_E is constant with respect of \mathcal{I}_p , the problem reduces to minimizing $\mathcal{L}_P + \mathcal{L}_R$, which can be written as follows:

$$\mathcal{L}_P + \mathcal{L}_R = \frac{1}{|\mathcal{I}_p|} \sum_{(k,l) \in \mathcal{I}_p} W_{kl}^P, \quad (16)$$

²In fact, most SGG methods do not perform a valid alignment and simply assign each entity node to the most overlapping ground truth, even though a ground truth node may be mapped to more than one output node.

Method	Supervision	SGGEN		PHRDET	
		R@50	R@100	R@50	R@100
VtransE [38]	Full	5.5	6.0	9.5	10.4
S-PPR-FCN [38]		6.0	6.9	10.6	11.1
VSPNET (Ours)		7.7	8.5	21.2	24.6
VtransE-MIL [38]	Weak	0.7	0.9	1.5	2.0
PPR-FCN [38]		1.5	1.9	2.4	3.2
VSPNET (Ours)		3.2	3.5	17.9	20.3

Table 1. Results on Visual Genome preprocessed by [38]. All numbers are in percentage.

where W^P is a pairwise cost function between output and target predicate nodes, measuring not only their semantic embedding distance, but also the discrepancy of their connectivity in graph. More specifically:

$$W_{kl}^P \triangleq \|P_k^O - P_l^T\|_2^2 + \frac{1}{n_r |\mathcal{I}_e|} \sum_{(i,j) \in \mathcal{I}_e} \sum_{r=1}^{n_r} \mathcal{X}(A_r^O[k, i], A_r^T[l, j]). \quad (17)$$

Note that the optimization of (16) is subject to (8), which makes $|\mathcal{I}_p|$ a constant. Hence, this problem is equivalent to maximum bipartite matching with fully connected cost function W^P , which can be solved in polynomial time using the Kuhn-Munkres algorithm [18].

Similarly, given \mathcal{I}_p , we can solve for \mathcal{I}_e , and repeat alternation. Every step leads to a lower or equal loss since either $\mathcal{L}_P + \mathcal{L}_R$ is minimized while \mathcal{L}_E is fixed, or $\mathcal{L}_E + \mathcal{L}_R$ is minimized while \mathcal{L}_P is fixed. Since \mathcal{L} cannot become negative, these iterations must converge. We have observed that the convergence value of \mathcal{L} is not sensitive to whether we start by initializing \mathcal{I}_e or \mathcal{I}_p , nor does it depend on the initialization value. In our experiments we initialize \mathcal{I}_p to an empty set and proceed with updating \mathcal{I}_e . We denote by v the number of iterations used for this alignment procedure.

4. Experiments

We apply our framework on the Visual Genome (VG) dataset [11] for the task of scene graph generation, and compare to both weakly and fully supervised baselines. Through quantitative and qualitative analysis, we show that VSPNET significantly outperforms the weakly supervised state of the art, and approaches fully supervised performance, while being five times faster than existing methods.

4.1. Implementation details

We use a region proposal network from an off-the-shelf Faster R-CNN [23] with an Inception-ResNet-v2 backbone [26] pretrained on the Open Images dataset [12]. For the attention models f_r , we used fully connected networks with two 2048-dimensional hidden layers and one single-dimensional output layer. For message passing, we used

a single fully connected layer of 2048 units for each of the three stages (*i.e.*, $g_r^{e \leftarrow}$, $g_r^{e \rightarrow}$, g^e , $g_r^{p \leftarrow}$, $g_r^{p \rightarrow}$, g^p). For predicting the final class embeddings from the entity and predicate states we used two separate fully connected networks each with a 2048-dimensional hidden layer and a 300-dimensional output layer which matches our word embedding dimension. All fully connected networks use leaky ReLU activation functions [6]. We used the original implementation of GRU [4] with 2048-dimensional states (d_e and d_p). Through cross-validation, we set $\lambda = 10$, $u = 3$, and $v = 3$.

The number of predicate nodes n_p is an important choice. Having more predicate nodes will increase recall and potentially reduce precision, or result in duplicate detection. Since SGG methods are conventionally evaluated at 100 and 50 predicates, we train our models with $n_p = 100$. To output only 50 predicates, we rank the predicate nodes with respect to their confidence, which is defined as the product of three classification confidence terms, subject, object and predicate. On the other hand, reducing the number of predicates will result in computational efficiency. We show in Section 4.4 that such reduction does not have an adverse effect on our results. We also report the performance of our method in the conventional supervised setting using a simple modification in our alignment procedure by adding a term in Eq 10 to maximize the overlap between the region proposal and ground truth bounding box.

4.2. Task Definition

The Visual Genome dataset consists of 108,077 images with manual annotation of objects and relationships, with open-vocabulary classes. [29] and [38] preprocess the annotated objects and relationships to produce scene graphs with a fixed vocabulary. [29] keeps 150 most frequent entity and 50 most frequent predicate classes, while [38] cuts at 200 and 100 respectively. We perform two sets of experiments, based on both [29] and [38], to be able to compare to the performances reported by each paper separately. We follow their preprocessing, data splits, and evaluation protocol, but we assume bounding boxes are not available during training.

The main evaluation metric dubbed SGGEN, measures

Method	Supervision	Time	SGGEN		SGCLS		PREDCLS	
			R@50	R@100	R@50	R@100	R@50	R@100
IMP [29]	Full	1.64	3.4	4.2	21.7	24.4	44.7	53.1
MSDN [14]		3.56	7.7	10.5	19.3	21.8	63.1	66.4
MotifNet [36]		N/A	6.9	9.1	23.8	27.2	41.8	48.8
Assoc. Emb. [19]		N/A	9.7	11.3	26.5	30.0	68.0	76.2
Graph R-CNN [30]		N/A	11.4	13.7	29.6	31.6	54.2	59.1
Factorizable Net [13]		0.55	N/A	N/A	N/A	N/A	N/A	N/A
VSPNET (Ours)	Weak	0.11	10.1	11.4	26.9	32.7	45.2	62.6
VSPNET (Ours)		0.11	4.8	5.5	25.5	30.4	44.3	59.8

Table 2. Results on VG preprocessed by [29]. Recall numbers are in percentage. Inference time is average number of seconds per image. Accuracy numbers for Factorizable Net are unknown because they report their numbers with a different VG preprocessing and split.

the accuracy of *subject-predicate-object* triplets. A detected triplet is considered correct if the predicted class for subject, object, and predicate are all correct, and the subject and object bounding boxes have an Intersection over Union (IoU) of at least 0.5 with ground truth. To evaluate, the top K triplets predicted by the model are matched to ground truth triplets. The number of correctly matched triplets is divided by the total number of triplets in the ground truth to compute recall@K. This value is averaged over all images, and following the literature, we report recall@50 and recall@100. SGGEN is highly affected by the quality of region proposals, if some ground truth objects do not match any proposal with $\text{IoU} > 0.5$, the model cannot reach 100% recall. Hence, SGCLS assumes ground truth bounding boxes are given at test time, instead of proposals. We also report PREDCLS which is like SGCLS but object classes are also given. Note that our method does not have a way to exploit the given object classes, so we do not expect to achieve superior performance on this metric. Finally, [38] evaluates using PHRDET, which stands for Phrase Detection. This metric is very similar to SGGEN, with the difference that instead of evaluating the bounding box of subject and object separately, the goal is to predict a union bounding box enclosing both the object and subject. To this end, we get the union box of predicted subject and object, and compare with the ground truth using IoU.

4.3. Results

Table 1 shows our quantitative results on VG following the preprocessing of [38]. Our VSPNET achieves the best weakly supervised performance over the only available baselines, with SGGEN performance more than two times higher and PHRDET more than six times higher than the state of the art. Moreover, it outperforms even supervised methods on the PHRDET measure. Furthermore, the supervised extension of our method also outperforms the supervised variants of those baselines.

To compare to more recent methods, we also perform experiments on the preprocessing used by [29], and closely

follow [30] for evaluation settings. We compare to all the state-of-the-art numbers reported by [30]. As illustrated in Table 2, our weakly supervised method significantly outperforms supervised methods such as [29] in SGGEN and [14] in SGCLS, while being an order of magnitude faster than both. Our fully supervised extension further improves the results, outperforming most of the recent fully supervised methods. Note that our method was not designed to extensively leverage full supervision, and hence it does not outperform all fully supervised methods. This is mainly because fully supervised methods train a Faster R-CNN directly on VG bounding boxes, while we used an off-the-shelf region proposal network that is not trained on VG, in both fully and weakly supervised versions of our method.

Furthermore, VSPNET has been designed for computational efficiency, and hence does not process all pairs of entities. Since all performance metrics are based on triplet recall, processing more pairs reduces the chance of missing a triplet, and increases the recall at the expense of more computation. In Table 2, we compare the inference time of our method with the statistics reported by [13], which is the only SGG method with a focus on computational complexity. We used identical settings (NVIDIA TITAN X, 200 proposals) to compute the average inference time per image over the entire test data. VSPNET is significantly faster than other methods, while having a competitive performance, due to our VSP reformulation and the novel role-driven message passing framework.

We observed that the PREDCLS performance varies a lot among recent methods, and is less correlated with the other metrics. For instance, while Graph R-CNN outperforms Associative Embedding in all other metrics, it is significantly worse in terms of PREDCLS. This is mostly due to the fact that some methods classify entities first, and utilize that to classify predicates, which means in the PREDCLS case where entities are given, they can use ground truth entities as an input to their model. Our method infers entities and predicates jointly which means we cannot utilize ground truth entity classes in the case of PREDCLS.

Alignment	Attention	u	n_p	SGGEN	
				R@50	R@100
Simple	2-layer	3	100	2.1	2.5
Iterative	1-layer	3	100	3.5	4.0
Iterative	2-layer	1	100	3.4	4.1
Iterative	2-layer	2	100	3.7	4.5
Iterative	2-layer	3	100	3.8	4.5
Iterative	2-layer	3	50	4.1	N/A

Table 3. Ablation study on VG preprocessed by [29]. u and n_p are the number of message passing steps and predicate nodes.

4.4. Ablation and Qualitative results

We analyze here how different parts of the proposed method contribute to the performance. First, we examine the effect of message passing by setting the number of message passing iterations u to 1, 2 and 3. Results reported in Table 3 suggest that at least two steps of message passing is necessary to obtain good results. Moreover, we compare our iterative alignment method to a naive one, where entity nodes and predicate nodes are independently aligned to minimize their pairwise embedding distance. Results show the significant impact of a global alignment where entity and predicates are interdependently aligned and their connectivity is taken into account. To illustrate the effectiveness of our attention module, we reduced the depth of its network from 2 to 1 layer, which resulted in a performance drop. Moreover, we show that a model trained with 50 predicate nodes can achieve a better R@50 than a model with 100 predicates and filtering less confident triplets. This means improving the efficiency by allocating less predicates actually improves the performance rather than hurting it.

We illustrate some randomly selected examples of our predicted graphs in Figure 3. We only visualize the most confident triplets, but do not remove mistakes. For instance, the first example shows that all most confident triplets connect the *woman* and *ski*, among all other proposals. Since VG has not been exhaustively cleaned, some annotations appear as *wears* while others are *wearing*, both being frequent enough to appear in the top 50 classes. This is why our model predicts both *wears* and *wearing* in all three examples. Furthermore, in the second example, there is a duplicate detection of *bike*, as two proposals both match fairly well the location of *bike*, and as our loss function do not penalize duplicates. The last example shows the predicate *man near man*, as we do not explicitly constrain predicates to be between two different entities.

5. Conclusion

We proposed a method to parse an image into a structured representation including entities, predicates, and their relationships. Our VSPNET does not require bounding boxes

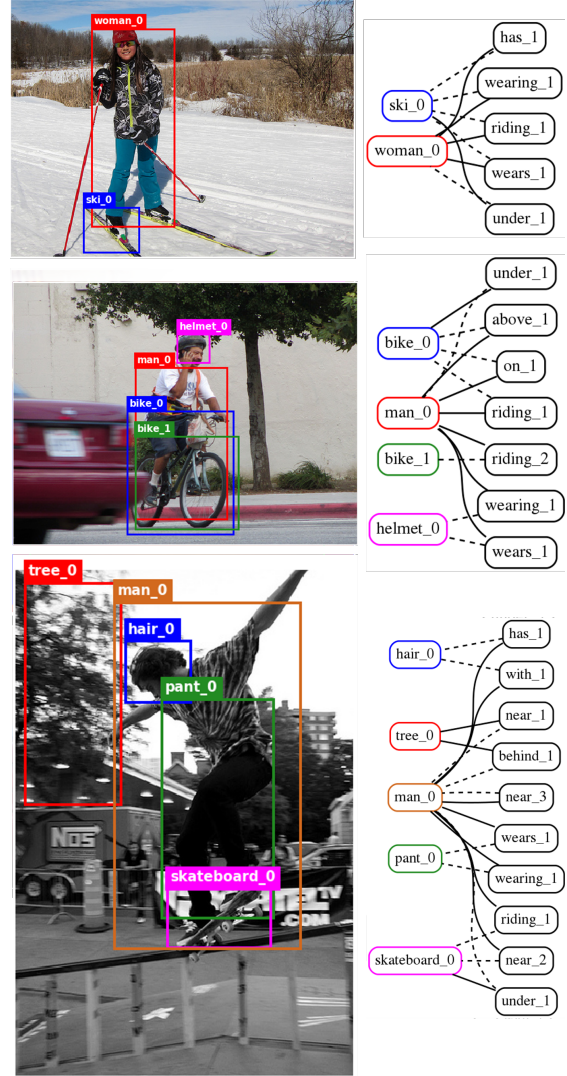


Figure 3. Examples of scene graphs generated by our VSPNET method. Solid and dashed lines represent subject and object roles respectively. Most confident triplets were shown only.

annotations for training, and does not rely on exhaustive processing of all region proposal pairs. To this end, we proposed a generalized formulation of SGG that disentangles predicates from entities, and enables sub-quadratic performance. Based on that, we proposed a novel graphical message passing framework with an attention-based, role-driven message routing module and a three-stage message aggregation network. We also proposed the first graph-based weakly supervised learning framework based on a novel graph alignment technique, which enables training without bounding annotations. We compared our method to the state of the art through extensive experiments, and achieved superior weakly supervised performance, and competitive supervised performance, while several times faster than other methods.

References

- [1] D. Bahdanau, K. Cho, and Y. Bengio. Neural machine translation by jointly learning to align and translate. *arXiv preprint arXiv:1409.0473*, 2014. 1
- [2] L. Banarescu, C. Bonial, S. Cai, M. Georgescu, K. Griffitt, U. Hermjakob, K. Knight, P. Koehn, M. Palmer, and N. Schneider. Abstract meaning representation for sembanking. In *Proceedings of the 7th Linguistic Annotation Workshop and Interoperability with Discourse*, pages 178–186, 2013. 1
- [3] X. Chen, L.-J. Li, L. Fei-Fei, and A. Gupta. Iterative visual reasoning beyond convolutions. In *Proceedings of the IEEE Conference on Computer Vision and Pattern Recognition*, pages 7239–7248, 2018. 2
- [4] K. Cho, B. Van Merriënboer, C. Gulcehre, D. Bahdanau, F. Bougares, H. Schwenk, and Y. Bengio. Learning phrase representations using rnn encoder-decoder for statistical machine translation. *arXiv preprint arXiv:1406.1078*, 2014. 4, 6
- [5] B. Dai, Y. Zhang, and D. Lin. Detecting visual relationships with deep relational networks. In *Proceedings of the IEEE Conference on Computer Vision and Pattern Recognition*, pages 3076–3086, 2017. 2
- [6] K. He, X. Zhang, S. Ren, and J. Sun. Delving deep into rectifiers: Surpassing human-level performance on imagenet classification. In *Proceedings of the IEEE international conference on computer vision*, pages 1026–1034, 2015. 6
- [7] S. Jae Hwang, S. N. Ravi, Z. Tao, H. J. Kim, M. D. Collins, and V. Singh. Tensorize, factorize and regularize: Robust visual relationship learning. In *Proceedings of the IEEE Conference on Computer Vision and Pattern Recognition*, pages 1014–1023, 2018. 2
- [8] J. Johnson, R. Krishna, M. Stark, L.-J. Li, D. Shamma, M. Bernstein, and L. Fei-Fei. Image retrieval using scene graphs. In *Proceedings of the IEEE conference on computer vision and pattern recognition*, pages 3668–3678, 2015. 1
- [9] K. Kato, Y. Li, and A. Gupta. Compositional learning for human object interaction. In *Proceedings of the European Conference on Computer Vision (ECCV)*, pages 234–251, 2018. 2
- [10] D. P. Kingma and J. Ba. Adam: A method for stochastic optimization. *arXiv preprint arXiv:1412.6980*, 2014. 5
- [11] R. Krishna, Y. Zhu, O. Groth, J. Johnson, K. Hata, J. Kravitz, S. Chen, Y. Kalantidis, L.-J. Li, D. A. Shamma, et al. Visual genome: Connecting language and vision using crowd-sourced dense image annotations. *International Journal of Computer Vision*, 123(1):32–73, 2017. 1, 6
- [12] A. Kuznetsova, H. Rom, N. Alldrin, J. Uijlings, I. Krasin, J. Pont-Tuset, S. Kamali, S. Popov, M. Mallocci, T. Duerig, et al. The open images dataset v4: Unified image classification, object detection, and visual relationship detection at scale. *arXiv preprint arXiv:1811.00982*, 2018. 6
- [13] Y. Li, W. Ouyang, B. Zhou, J. Shi, C. Zhang, and X. Wang. Factorizable net: an efficient subgraph-based framework for scene graph generation. In *Proceedings of the European Conference on Computer Vision (ECCV)*, pages 335–351, 2018. 2, 7
- [14] Y. Li, W. Ouyang, B. Zhou, K. Wang, and X. Wang. Scene graph generation from objects, phrases and region captions. In *Proceedings of the IEEE International Conference on Computer Vision*, pages 1261–1270, 2017. 2, 7
- [15] X. Liang, L. Lee, and E. P. Xing. Deep variation-structured reinforcement learning for visual relationship and attribute detection. In *Proceedings of the IEEE conference on computer vision and pattern recognition*, pages 848–857, 2017. 2
- [16] Y. Liu, R. Wang, S. Shan, and X. Chen. Structure inference net: object detection using scene-level context and instance-level relationships. In *Proceedings of the IEEE Conference on Computer Vision and Pattern Recognition*, pages 6985–6994, 2018. 2
- [17] C. Lu, R. Krishna, M. Bernstein, and L. Fei-Fei. Visual relationship detection with language priors. In *European Conference on Computer Vision*, pages 852–869. Springer, 2016. 2
- [18] J. Munkres. Algorithms for the assignment and transportation problems. *Journal of the society for industrial and applied mathematics*, 5(1):32–38, 1957. 6
- [19] A. Newell and J. Deng. Pixels to graphs by associative embedding. In *Advances in neural information processing systems*, pages 2171–2180, 2017. 2, 7
- [20] J. Peyre, J. Sivic, I. Laptev, and C. Schmid. Weakly-supervised learning of visual relations. In *Proceedings of the IEEE International Conference on Computer Vision*, pages 5179–5188, 2017. 2
- [21] B. A. Plummer, A. Mallya, C. M. Cervantes, J. Hockenmaier, and S. Lazebnik. Phrase localization and visual relationship detection with comprehensive image-language cues. In *Proceedings of the IEEE International Conference on Computer Vision*, pages 1928–1937, 2017. 2
- [22] S. Qi, W. Wang, B. Jia, J. Shen, and S.-C. Zhu. Learning human-object interactions by graph parsing neural networks. In *Proceedings of the European Conference on Computer Vision (ECCV)*, pages 401–417, 2018. 2
- [23] S. Ren, K. He, R. Girshick, and J. Sun. Faster r-cnn: Towards real-time object detection with region proposal networks. In *Advances in neural information processing systems*, pages 91–99, 2015. 1, 3, 6
- [24] A. Sharma, N. H. Vo, S. Aditya, and C. Baral. Towards addressing the winograd schema challengebuilding and using a semantic parser and a knowledge hunting module. In *Twenty-Fourth International Joint Conference on Artificial Intelligence*, 2015. 1
- [25] J. Shi, H. Zhang, and J. Li. Explainable and explicit visual reasoning over scene graphs. *arXiv preprint arXiv:1812.01855*, 2018. 1
- [26] C. Szegedy, S. Ioffe, V. Vanhoucke, and A. A. Alemi. Inception-v4, inception-resnet and the impact of residual connections on learning. In *Thirty-First AAAI Conference on Artificial Intelligence*, 2017. 6
- [27] D. Teney, L. Liu, and A. van den Hengel. Graph-structured representations for visual question answering. In *Proceedings of the IEEE Conference on Computer Vision and Pattern Recognition*, pages 1–9, 2017. 1

- [28] S. Woo, D. Kim, D. Cho, and I. S. Kweon. Linknet: Relational embedding for scene graph. In *Advances in Neural Information Processing Systems*, pages 558–568, 2018. [2](#)
- [29] D. Xu, Y. Zhu, C. B. Choy, and L. Fei-Fei. Scene graph generation by iterative message passing. In *Proceedings of the IEEE Conference on Computer Vision and Pattern Recognition*, pages 5410–5419, 2017. [2](#), [6](#), [7](#), [8](#)
- [30] J. Yang, J. Lu, S. Lee, D. Batra, and D. Parikh. Graph rcnn for scene graph generation. In *Proceedings of the European Conference on Computer Vision (ECCV)*, pages 670–685, 2018. [2](#), [7](#)
- [31] M. Yatskar, L. Zettlemoyer, and A. Farhadi. Situation recognition: Visual semantic role labeling for image understanding. In *Proceedings of the IEEE Conference on Computer Vision and Pattern Recognition*, pages 5534–5542, 2016. [3](#)
- [32] G. Yin, L. Sheng, B. Liu, N. Yu, X. Wang, J. Shao, and C. Change Loy. Zoom-net: Mining deep feature interactions for visual relationship recognition. In *Proceedings of the European Conference on Computer Vision (ECCV)*, pages 322–338, 2018. [2](#)
- [33] R. Yu, A. Li, V. I. Morariu, and L. S. Davis. Visual relationship detection with internal and external linguistic knowledge distillation. In *Proceedings of the IEEE International Conference on Computer Vision*, pages 1974–1982, 2017. [2](#)
- [34] Y. Yuan, X. Liang, X. Wang, D.-Y. Yeung, and A. Gupta. Temporal dynamic graph lstm for action-driven video object detection. In *Proceedings of the IEEE International Conference on Computer Vision*, pages 1801–1810, 2017. [2](#), [3](#)
- [35] R. Zellers, Y. Bisk, A. Farhadi, and Y. Choi. From recognition to cognition: Visual commonsense reasoning. *arXiv preprint arXiv:1811.10830*, 2018. [1](#)
- [36] R. Zellers, M. Yatskar, S. Thomson, and Y. Choi. Neural motifs: Scene graph parsing with global context. In *Proceedings of the IEEE Conference on Computer Vision and Pattern Recognition*, pages 5831–5840, 2018. [2](#), [7](#)
- [37] H. Zhang, Z. Kyaw, S.-F. Chang, and T.-S. Chua. Visual translation embedding network for visual relation detection. In *Proceedings of the IEEE conference on computer vision and pattern recognition*, pages 5532–5540, 2017. [2](#)
- [38] H. Zhang, Z. Kyaw, J. Yu, and S.-F. Chang. Ppr-fcn: weakly supervised visual relation detection via parallel pairwise rfcn. In *Proceedings of the IEEE International Conference on Computer Vision*, pages 4233–4241, 2017. [2](#), [6](#), [7](#)
- [39] B. Zhuang, L. Liu, C. Shen, and I. Reid. Towards context-aware interaction recognition for visual relationship detection. In *Proceedings of the IEEE International Conference on Computer Vision*, pages 589–598, 2017. [2](#)